# Optimization of hyaluronic acid-tyramine/silk-fibroin composite hydrogels for cartilage tissue engineering and delivery of anti-inflammatory and anabolic drugs



**Author(s):**
Ziadlou, Reihane; Rotman, Stijn; Teuschl, Andreas; Salzer, Elias; Barbero, Andrea; Martin, Ivan; Alini, Mauro; Eglin, David; Grad, Sibylle

**Publication date:**
2021-01

**Permanent link:**
https://doi.org/10.3929/ethz-b-000468394



**Originally published in:**
Biomaterials Advances 120, https://doi.org/10.1016/j.msec.2020.111701

Materials Science & Engineering C 120 (2021) 111701

Contents lists available at ScienceDirect

Materials Science & Engineering C

journal homepage: www.elsevier.com/locate/msec

# Optimization of hyaluronic acid-tyramine/silk-fibroin composite hydrogels for cartilage tissue engineering and delivery of anti-inflammatory and anabolic drugs

Reihane Ziadlou [a,b], Stijn Rotman [a], Andreas Teuschl [d], Elias Salzer [d,e], Andrea Barbero [b], Ivan Martin [b,c], Mauro Alini [a], David Eglin [a], Sibylle Grad [a,f,*]

[a] AO Research Institute Davos, Davos Platz 7270, Switzerland
[b] Department of Biomedical Engineering, University of Basel, Allschwil 4123, Switzerland
[c] Department of Biomedicine, University Hospital Basel, University of Basel, Basel 4001, Switzerland
[d] Department of Biochemical Engineering, University of Applied Sciences Technikum Wien, 1200 Vienna, Austria
[e] Orthopaedic Biomechanics, Department of Biomedical Engineering, Eindhoven University of Technology, 5600 MB Eindhoven, The Netherlands
[f] Department of Health Sciences and Technology, ETH Zürich, Zürich 8092, Switzerland

ARTICLE INFO

*Keywords:*
Hydrogel
Hyaluronic acid-tyramine
Silk-fibroin
Enzymatic cross-linking
Chondrocytes
Tissue engineering
Drug delivery
Mechanical testing
Cartilage

ABSTRACT

Injury of articular cartilage leads to an imbalance in tissue homeostasis, and due to the poor self-healing capacity of cartilage the affected tissue often exhibits osteoarthritic changes. In recent years, injectable and highly tunable composite hydrogels for cartilage tissue engineering and drug delivery have been introduced as a desirable alternative to invasive treatments. In this study, we aimed to formulate injectable hydrogels for drug delivery and cartilage tissue engineering by combining different concentrations of hyaluronic acid-tyramine (HA-Tyr) with regenerated silk-fibroin (SF) solutions. Upon enzymatic crosslinking, the gelation and mechanical properties were characterized over time. To evaluate the effect of the hydrogel compositions and properties on extracellular matrix (ECM) deposition, bovine chondrocytes were embedded in enzymatically crosslinked HA-Tyr/SF composites (in further work abbreviated as HA/SF) or HA-Tyr hydrogels. We demonstrated that all hydrogel formulations were cytocompatible and could promote the expression of cartilage matrix proteins allowing chondrocytes to produce ECM, while the most prominent chondrogenic effects were observed in hydrogels with HA20/SF80 polymeric ratios. Unconfined mechanical testing showed that the compressive modulus for HA20/SF80 chondrocyte-laden constructs was increased almost 10-fold over 28 days of culture in chondrogenic medium which confirmed the superior production of ECM in this hydrogel compared to other hydrogels in this study. Furthermore, in hydrogels loaded with anabolic and anti-inflammatory drugs, HA20/SF80 hydrogel showed the longest and the most sustained release profile over time which is desirable for the long treatment duration typically necessary for osteoarthritic joints. In conclusion, HA20/SF80 hydrogel was successfully established as a suitable injectable biomaterial for cartilage tissue engineering and drug delivery applications.

## 1. Introduction

Articular cartilage (AC) is a highly structured and hydrated functional tissue with remarkable load-bearing properties that facilitate smooth and painless movement of joints. Chondrocytes in AC are surrounded by a self-produced tissue specific extracellular matrix (ECM) that is mainly composed of collagen type II, aggrecan and other proteoglycans. Because of the avascular nature of cartilage, slow matrix turnover rate and low cell density, the intrinsic healing capacity of articular cartilage is minimal [1,2]. Injury of articular cartilage leads to an imbalance in tissue homeostasis which is associated with a high risk of progressing towards osteoarthritis (OA). OA, or degenerative joint disease, is the major cause of disability in the elderly population [3–5]. Conventional treatment approaches for cartilage repair including autologous chondrocyte implantation (ACI), microfracture treatments, total joint arthroplasty and allografts, all have several short and long term limitations [6–9]. A different approach for prevention or treatment of OA could involve locally injectable hydrogels that can be utilized in

* Corresponding author at: AO Research Institute Davos, Davos Platz 7270, Switzerland.
*E-mail address:* sibylle.grad@aofoundation.org (S. Grad).

https://doi.org/10.1016/j.msec.2020.111701
Received 19 June 2020; Received in revised form 21 October 2020; Accepted 2 November 2020
Available online 5 November 2020

two distinct strategies. First, hydrogels can be used for local delivery of drugs with anti-catabolic and anabolic effects to create a beneficial environment for cartilage regeneration. Secondly, hydrogels can serve as scaffold material for cartilage tissue engineering (TE) approaches in which chondrocytes are being embedded within the hydrogel and then injected at the site of damage. Hydrogels are materials of high water content, similar to articular cartilage ECM and are widely used for cartilage TE and drug delivery purposes [10–12]. Due to the hydrophilic nature of hydrogels, they are permeable for oxygen and nutrients which are necessary factors for cell proliferation and phenotypic behaviour in 3D microenvironments [13].

Several hydrogels from natural polymers, such as hyaluronic acid (HA), agarose, alginate and collagen have been used for 3D culture of chondrocytes [14–19]. HA is a major component of articular cartilage ECM and is present in the synovial fluid, interacting biologically and mechanically within the water rich environment. HA has been introduced as a biodegradable, non-immunogenic and non-inflammatory polysaccharide which can promote maintenance of the chondrogenic phenotype and ECM synthesis of embedded cells [20–24]. To establish a HA-based hydrogel, HA polymers need to be functionalized with crosslinking groups. In several studies tyramine (Tyr) modified HA (HA-Tyr) has been introduced as an enzymatically crosslinked hydrogel for drug delivery and TE applications [25–28]. It is known that cells can bind to, proliferate and spread in HA-Tyr via HA-binding cell-surface proteins which makes it a suitable material for cell encapsulation and TE applications [29,30]. Nevertheless, HA-Tyr based hydrogels are relatively fast degradable in presence of physiological levels of hyaluronidase, depending on Tyr degree of substitution and $H_2O_2$ concentration during crosslinking [26,30]. It was shown that with increasing concentrations of $H_2O_2$ and horseradish peroxidase (HRP), stiffer hydrogels which are less degradable could be produced [30,31]. However, high concentrations of HRP and $H_2O_2$ will increase cytotoxicity and potentially induce immune responses [32,33]. Also, by encapsulating high numbers of cells in HA-Tyr hydrogels, their mechanical properties were significantly decreased (storage modulus ˂1 kPa), which is not sufficient for maintaining the chondrogenic phenotype and matrix production [31,34–38]. Thus, HA-Tyr hydrogels can benefit from a composite system that improves mechanical properties and reduces the degradation rate.

Silk-fibroin (SF) protein derived from *Bombyx mori* (*B. mori*) cocoons can form biocompatible hydrogels with adequate mechanical strength and slow rate of degradation, which makes it a suitable biomatrix for long-term cell culture and cartilage regeneration [39–42]. However, due to the slow gelation of SF upon enzymatic crosslinking and lack of cell specific epitopes for cell adhesion, clinical cell-laden applications are not feasible [43–45]. In addition, crystallization and self-assembly of the SF polymers leading to significant changes in mechanical properties were reported [46]. Previously, several composite hydrogels with SF showed great potential for wide ranges of applications, including stem cell encapsulations, cell therapies after myocardial infarction, or bone tissue engineering [43,47–49]. A composite hydrogel comprising of HA-Tyr and SF (HA/SF) has the potential to preserve the superior properties of both hydrogels, but also to diminish their previously described weaknesses [42]. Due to the presence of Tyr in HA-Tyr and tyrosine in the heavy chain of SF, enzymatic crosslinking of the composite hydrogels leads to the formation of covalently crosslinked gels with di-tyramine, di-tyrosine and tyramine-tyrosine bonds [50]. Raia et al. showed that the enzymatic crosslinking of composite HA/SF hydrogels could provide a controllable gelation and degradation with a possibility to tune stiffness and viscoelasticity by changing the HA-Tyr concentration and thus the polymeric HA/SF ratio, providing a platform for TE and drug delivery applications [50]. It was previously reported that injection of the enzymatically crosslinkable HA-Tyr encapsulated with an anti-inflammatory drug (dexamethasone), could successfully reduce inflammation in animal models of arthritis [25,28]. Also, SF has previously been used as an injectable material for sustained drug delivery applications [39]. Therefore, with the clinical application in mind, the injectability and the anti-inflammatory properties credited to HA and SF materials make them advantageous to serve as a delivery system for either cells and/or small molecules for cartilage regeneration [20,51].

In this study, we hypothesized that by combining different concentrations of HA-Tyr with regenerated aqueous SF solutions, a tunable and injectable hydrogel for cartilage TE and drug delivery purposes could be formulated. Articular chondrocytes embedded in HA/SF composite hydrogels were assessed in terms of cell viability, phenotypic behaviour and ECM production. Upon enzymatic crosslinking with HRP and $H_2O_2$, the gelation and mechanical properties were characterized over time. As a proof of principle, to demonstrate the feasibility of releasing drugs, we also showed the effect of HA/SF hydrogel composition on the release of small hydrophobic anti-inflammatory and anabolic drugs, that had previously been identified as promising agents. Our findings highlight the potential of HA/SF hydrogels for application in cartilage regeneration.

## 2. Materials and methods

### 2.1. HA-Tyr synthesis

To synthesize HA-Tyr, the carboxyl groups of HA were substituted with Tyr through an amidation procedure, using a previously established protocol [52]. Briefly, sodium hyaluronate from *Streptococcus equi* (Contipro Biotechs.r.o., Czech Republic) with average molecular weight of 290 kDa was dissolved in deionized $H_2O$ (10 mg/mL). Tyr conjugation to HA was catalyzed by adding 5 mmol 4-(4,6-dimethoxy-1,3,5-triazin-2-yl)-4-methylmorpholinium chloride (DMTMM) (TCI Europe N.V.) coupling agent followed by 5 mmol Tyr (Sigma-Aldrich, St. Louis, MO), which was slowly added to the reaction. The reaction occurred at 37 °C under continuous stirring for 24 h. The HA-Tyr product was precipitated by adding 8% *v*/v saturated sodium chloride solution and a three-fold volume of 96% ethanol. After several washing steps with aqueous solutions containing increasing ethanol concentrations (up to 100% ethanol), the product was filtered and dried under vacuum for 48 h. The amidation reaction was repeated to increase the degree of substitution (DS) to a final value of 14% ($DS_{mol}$ in percent). The degree of tyramine hydrochloride substitution of HA-Tyr was determined with proton nuclear magnetic resonance spectroscopy ($^1$H NMR) and ultraviolet−visible spectroscopy (UV–vis) measurements. HA-Tyr products were stored at room temperature and obscured from light until further use.

### 2.2. Preparation of silk-fibroin solution

Using silk cocoons from *B. mori* silkworm, 8% aqueous silk solutions were prepared according to the protocol described elsewhere [41]. Briefly, sericin protein was removed from *B. mori* silkworm cocoons to prevent potential immunogenic host reactions. To achieve this, cocoons were degummed by placing 5 g of cleaned and cut cocoons in 2 L of a boiling 0.02 M sodium carbonate ($Na_2CO_3$) solution (Sigma-Aldrich, St. Louis, MO) for 30 min, with manual stirring every 10 min. Degummed SF was washed several times in distilled $H_2O$ and dried overnight at room temperature. After weighing the dried degummed SF, 35–40% of the weight was lost which is expected due to the sericin protein removal. The SF was dissolved in 9.3 M aqueous LiBr solution at 60 °C for 4 h, yielding a 20 *w*/*v*% solution. Throughout this process, the solution was stirred every 30 min. Subsequently, the solution was dialyzed against demineralized $H_2O$ using a Slide-a-Lyzer dialysis cassette (MWCO 3500; Thermo Fisher Scientific, Inc., Rockford, IL) for 48 h exchanging the water several times. After centrifugation, the final concentration of SF aqueous solution was determined by weighing air dried samples and adjusted to 8% *w*/v.

### 2.3. Preparation of HA/SF hydrogels

HA-Tyr (DS = 14%) was dissolved at a final concentration of 30 mg/mL in ultrapure distilled water overnight at 4 °C under agitation. SF solution (80 mg/mL) and HA-Tyr (30 mg/mL) were mixed with ultrapure water by means of gentle pipetting to acquire a final SF concentration of 20 mg/mL and a final HA concentrations of 1.05, 2.22, and 5 mg/mL. The final compositions of the composite precursor hydrogels are listed in Table 1. Crosslinking of the precursor hydrogels occurred at 37 °C and was initiated by adding 10 U/mL of aqueous HRP solution, followed by addition of 0.01% $H_2O_2$ to a final molarity of 3.2 mM (both from Sigma-Aldrich, St. Louis, MO). Henceforth, samples are named according to the ratio of HA-Tyr and SF non-crosslinked precursor hydrogels as defined in Table 1.

### 2.4. Rheological measurements and gelation time

Rheological measurements were performed to investigate the viscoelastic properties of the hydrogels, using an Anton Paar MCR-302 rheometer equipped with a Peltier temperature control unit. The experiments were performed at 37 °C on the rheometer using a 25 mm stainless steel upper cone and Peltier bottom plate to perform oscillatory and rotational tests (time sweep and strain sweep). The hydrogel precursors were mixed with HRP as described, loaded onto the plate, and subsequently, after lowering the cone, $H_2O_2$ was added into the gap. To prevent evaporation during analysis, an oil layer was deployed around the system. The storage modulus (G′) and loss modulus (G″) of the hydrogels were measured at 1 Hz with a strain of 1%, until a plateau value was reached. After allowing for complete gelation with time sweep test, strain sweeps between 0.1%–500% at 1 Hz were applied (amplitude sweep). Furthermore, the gelation time was evaluated by vial inversion test. For this respect, the enzymatic crosslinking of the hydrogels was initiated by adding $H_2O_2$ into the vials while they were kept and monitored at 37 °C. The time at which the solution was gelled and was not flowing after the vial inversion was considered as the gelation time.

### 2.5. Cell-laden constructs

For preparation of the cell-laden hydrogels, chondrocytes were harvested from articular cartilage of fetlock joints of young calves as previously described [53]. Briefly, after cutting the tissues with a scalpel into small pieces in a sterile environment, they were pre-digested with 0.1% Pronase (Roche, Switzerland) and subsequently digested with 600 U/mL Collagenase II (BioConcept, Switzerland) in Dulbecco's modified Eagle medium (DMEM) by overnight stirring in a spinner flask at 37 °C, 5% $CO_2$. The isolated chondrocytes were expanded for one passage to reach 80% confluency in basal medium (BM) containing high glucose DMEM supplemented with 1 mM sodium pyruvate, 10 mM HEPES, 1% penicillin/streptomycin (P/S), 10% fetal bovine serum (FBS) (all from Gibco, UK), 1 ng/mL transforming growth factor (TGF)-ß1 and 5 ng/mL fibroblast growth factor-2 (FGF-2) (both from Fitzgerald) in a humidified incubator (37 °C, 5% $CO_2$). For cell encapsulation, chondrocytes of passage 1 were suspended in culture medium and were embedded at a final concentration of 20 × $10^6$ cells/mL in the non-crosslinked precursor hydrogel formulations mentioned in Table 1. After dispersion of the cells in the precursor hydrogel (as explained in Section 2.3), enzymatic crosslinking was initiated by adding 0.01% $H_2O_2$ in a humidified incubator (37 °C, 5% CO2). The 3D cell-scaffold constructs were cultured for up to 28 days in standard chondrogenic medium containing BM supplemented with 1.25 mg/mL human serum albumin (Gibco, UK), ITS- Premix (Corning, USA), 0.1 mM ascorbic acid 2-phosphate (Sigma-Aldrich, St. Louis, MO, USA), 1% P/S, 10 ng/mL TGF-β1 and $10^{-7}$ M dexamethasone (Sigma-Aldrich, USA) or in chondro-permissive medium which was composed of chondrogenic medium without TGF-β1. The experiments were performed on three replicates of two independent bovine donors.

**Table 1**
Sample precursor compositions. Samples are reported by the mass percent of HA-Tyramine (HA-Tyr), while the silk-fibroin (SF) concentration in all samples containing SF is constant (20 mg/mL). All samples were crosslinked at 37 °C with 10 U/mL of HRP, followed by 0.01% $H_2O_2$ (3.2 mM).

| Sample name | Final HA-Tyr concentration (mg/mL) | Final SF concentration (mg/mL) |
|---|---|---|
| *HA100/SF0* | 5 | 0 |
| *HA20/SF80* | 5 | 20 |
| *HA10/SF90* | 2.22 | 20 |
| *HA5/SF95* | 1.05 | 20 |
| *HA0/SF100* | 0 | 20 |

### 2.6. Cell viability after encapsulation in the hydrogels

The viability of the cells encapsulated in the hydrogels was assessed at 24 h, 72 h and 7 days using a live/dead (L/D) assay, where living cells are stained with calcein-AM (Ca-AM), and dead cells with ethidium homodimer-1 (EthD-1) (both from Sigma-Aldrich, St. Louis, MO). Hydrogel discs (2 mm in height) were prepared with a biopsy punch of 4 mm in diameter. After three washes with phosphate buffered saline (PBS), the discs were protected from light and incubated in a staining solution containing 10 μM Ca-AM and 1 μM EthD-1 in serum-free high glucose DMEM in a humidified incubator (37 °C, 5% $CO_2$) for 90 min. The hydrogels were imaged with a confocal laser scanning microscope (LSM510, Zeiss), where both single plane and *Z*-stack images were acquired. For quantification of the cell viability, three different fields of view were imaged which were counted and quantified with ImageJ/Fiji.

### 2.7. Mechanical testing

Unconfined compression tests were performed on an Instron 5866 electromechanical test instrument equipped with a 10 N load cell. Cell encapsulated hydrogels were tested after 3, 7, 14, 21 and 28 days of culture in chondrogenic medium. The hydrogels (4 mm in diameter; ~2 mm in height) were placed between stainless steel parallel plates through which after a pre-load, three cycles of loading-unloading to 20% strain were applied. A strain rate of 0.667% per second was implemented and the compressive modulus and hysteresis were calculated between 5% and 10% strain in the second cycle of loading-unloading for each sample, to ensure there were no measurement artefacts. Subsequently, strain was held constant at 20% and stress relaxation tests were performed for a duration of 600 s. Using Python software, the compressive modulus and the percentage of the relaxation were determined in four replicates.

### 2.8. RNA extraction and gene expression analysis

For total RNA extraction from cell-seeded hydrogels at days 0 (monolayer culture at passage 1), 3, 7 and 21 of chondrogenic culture, 1 mL of TRI reagent (Molecular Research Center) was added to the scaffolds and the constructs were homogenized by a Tissue Lyser (Qiagen, Hilden, Germany) for 5 min at 5 Hz. Subsequently, the RNA was extracted using phase separation by 1-bromo-3-chloropropane (Sigma-Aldrich, St. Louse, MO, USA) in a volume ratio of 1:10 with the TRI reagent. The quantity and quality of the RNA samples were measured with a nano-photometer (Nanodrop, Thermo Scientific). cDNA synthesis was performed with 1 μg of total RNA sample, random hexamer primers and TaqMan™ reverse transcription reagents (Applied Biosystems, Carlsbad, CA, United States). Quantitative real-time PCR (qPCR) was carried out using TaqMan™ Universal Master Mix (Applied Biosystems, Foster City, CA, USA), and the Quant Studio 6 Flex instrument and software (Applied Biosystems) were used for detection. The gene expression assays and primer sequences for *bovine* ribosomal protein lateral stalk subunit P0 (*RPLP0*), aggrecan (*ACAN*), collagen type II

alpha 1 chain (*COL2A1*), collagen type I alpha 2 chains (*COL1A2)*, SRY-Box Transcription Factor 9 (*SOX-9*), cartilage oligomeric matrix protein (*COMP*), matrix metalloproteinase 1 (*MMP1*) and interleukin 6 (*IL-6*) are shown in Table 2. The relative gene expression was calculated using the $2^{-\Delta\Delta CT}$ quantification method [54], with *RPLP0* as endogenous control. The gene expression was normalized to the expression level of the day 0 monolayer culture to quantify the effects of 3D cell culture in HA/SF hydrogels.

### 2.9. Histology and immunohistochemistry

Hydrogel discs were prepared with a biopsy punch of 4 mm in diameter at days 1, 14, 21 and 28. The discs were washed with PBS and fixed in 4% formaldehyde overnight at 4 °C. Subsequently, the discs were washed 3 times in PBS and incubated overnight in 5% sucrose solution at 4 °C. Then, the samples were embedded in cryo-compound and were sectioned with a cryostat at 8 μm thickness. To visualize cells, collagen and proteoglycan deposition, hematoxylin-eosin (HE), nuclear fast red stain, Safranin-O/Fast green and Alcian blue staining were performed. For Safranin-O/Fast green staining, the slides were first incubated with Weigert's Hematoxylin for 10 min; then, the sections were stained with 0.02% Fast green in ultrapure (ddH2O) water for 5 min to reveal collagen deposition. Subsequently, the sections were stained with 0.1% Safranin-O solution for 12 min, to reveal proteoglycan deposition, followed by sequential differentiation in 70%, 96% and 100% ethanol. For Alcian blue staining, the proteoglycans were stained with Alcian blue solution in acidic pH for 30 min. Afterwards, the slides were counterstained with nuclear fast red stain (Sigma) for nuclear staining.

The presence of collagen type II (COL-II) was identified immunohistochemically using a monoclonal antibody against COL-II (CIIC1; 2 μg/mL IgG, Developmental Studies Hybridoma Bank, University of Iowa). Briefly, after enzyme treatment with 25 mg/mL hyaluronidase and 0.25 U/mL chondroitinase ABC (Sigma-Aldrich, St. Louse, MO, USA) at 37 °C for 30 min, non-specific binding sites were blocked with horse serum (Vector Laboratories, Burlingame, CA, USA) for 1 h at RT.

**Table 2**
Oligonucleotide primers and probes and assays (*bovine*) used for quantitative real-time PCR.

| Gene | Primer/probe type | Sequence/assay |
|---|---|---|
| *ACAN* | Primer forward (5′-3′)<br>Primer reverse (5′-3′)<br>Probe (5′ FAM/3′ TAMRA) | CCA ACG AAA CCT ATG ACG TGT ACT<br>GCA CTC GTT GGC TGC CTC ATG TTG<br>CAT AGA AGA CCT CGC CCT CCA |
| *COL2A1* | Primer forward (5′-3′)<br>Primer reverse (5′-3′)<br>Probe (5′ FAM/3′ TAMRA) | AAG AAA CAC ATC TGG TTT GGA GAA A<br>TGTTTGGAGTGGGTTTCAGAAATA<br>CAA CGG TGG CTT CCA CTT CAG CTA TGG |
| *COL1A2* | Primer forward (5′-3′)<br>Primer reverse (5′-3′)<br>Probe (5′ FAM/3′ TAMRA) | TGC AGT AAC TTC GTG CCT AGC A<br>CGC GTG GTC CTC TAT CTC CA<br>CAT GCC AAT CCT TAC AAG AGG CAA CTG C |
| *COMP* | Primer forward (5′-3′)<br>Primer reverse (5′-3′)<br>Probe (5′ FAM/3′ TAMRA) | CCA GAA GAA CGA CGA CCA GAA<br>TCT GAT CTG AGT TGG GCA CCT T<br>ACG GCG ACC GGA TCC GCA A |
| *MMP1* | Primer forward (5′-3′)<br>Primer reverse (5′-3′)<br>Probe (5′ FAM/3′ TAMRA) | TTC AGC TTT CTC AGG ACG ACA TT<br>CGA CTG GCT GAG TGG GAT TT<br>TCC AGG CCA TCT ACG GAC CTT CCC |
| *IL-6* | Primer forward (5′-3′)<br>Primer reverse (5′-3′)<br>Probe (5′ FAM/3′ TAMRA) | TTC CAA AAA TGG AGG AAA AGG A<br>TCC AGA AGA CCA GCA GTG GTT<br>TCC AGA AGA CCA GCA GTG GTT |
| *RPLP0* | 5′ FAM-3′ NFQ | Bt03218086_m1 |

*ACAN:* aggrecan; *COL2A1*: collagen type II; *COL1A2*: collagen type I*; COMP:* cartilage oligomeric matrix protein; *MMP1*: matrix metalloproteinase 1; *IL-6*: interleukin 6; FAM: carboxyfluorescein; TAMRA: tetramethylrhodamine.

After incubation with the primary antibody at 4 °C overnight, the protein was detected using a secondary biotinylated anti-*mouse* antibody (Vector Laboratories) followed by incubation with avidin-biotin-peroxidase complex (Vectastain ABC Kit, *mouse* IgG, Vector Laboratories). Peroxidase activity was visualized using diaminobenzidine (DAB) as a substrate (ImmPACT DAB, Substrate for Peroxidase, Vector Laboratories).

### 2.10. Drug encapsulation and release study

HA100/SF0, HA20/SF80 and HA10/SF90 hydrogels were loaded with 1 mM of Vanillic acid (VA) or Epimedin C (Epi C), which both showed anti-catabolic and anabolic effects on human chondrocytes in a previous screening study performed by the authors [55]. The drug loaded constructs were prepared by mixing 1 mM of small molecules with hydrogel precursors as explained in Section 2.3. Enzymatic cross-linking was initiated following addition of 3.2 mM $H_2O_2$ to 1 mL precursor hydrogel and the gelation was proceeded at 37 °C in a microtube. After gelation, 500 μL of PBS were added to each hydrogel for the drug release. To quantify the drug release, 10 μL of the aspirated release media were injected into a high-pressure liquid chromatography (HPLC) device (Agilent 1200) with a C18 column. For VA release media, the mobile phase consisted of acetonitrile/0.5% acetic acid (12:88 *v*/v), and for Epi C release media, the mobile phase was acetonitrile/water (30:70 v/v). VA was detected by UV absorption at 260 nm and Epi C at 270 nm. The flowrate of the mobile phase was consistent at 1 mL/min. With the described protocol, peaks for VA and Epi C were detected approximately 6 min and 5 min after sample injection. Standard curves of VA and Epi C in PBS were used to correlate HPLC detection peaks with drug concentration of the release media. After 60 days, the hydrogels were digested in 1 mL of an enzyme cocktail containing hyaluronidase (Sigma-Aldrich, St. Louis, MO), and protease (Pronase, Sigma-Aldrich, St. Louis, MO) dissolved at 1 U/mL and 0.001 U/mL in PBS, respectively.

### 2.11. Statistical analysis

Statistical comparisons were performed using Graphpad Prism 8. One-way analysis of variance (ANOVA) followed by Tukey's post hoc test (multiple comparison) was applied as non-parametric test of three independent experiments with different *bovine* chondrocyte donors. To evaluate statistical significance among the groups, differences were considered statistically significant at $p < 0.05$.

## 3. Results

### 3.1. Hydrogel gelation

Different concentrations of HA-Tyr were mixed with SF to characterize gelation and mechanical properties over time. Possible cross-linking sites in the composite hydrogel systems comprise di-tyramine between hyaluronan macromolecules, di-tyrosine between fibroin proteins and tyramine-tyrosine bonds between hyaluronan and fibroin (Fig. 1A). The molecular weight of the HA backbone was 290 kDa and the repeating unit has a weight of 0.403 kDa; thus, the HA backbone consists of 719 repeating units. The degree of substitution of tyramine was 14%; therefore, 101 tyramine units were present per HA molecule. As we had different HA-Tyr concentrations in our composite hydrogels, the tyramine concentration ranged from 1.74 μM at a HA-Tyr concentration of 5 mg/mL, to 0.37 μM at a HA-Tyr concentration of 1.05 mg/mL.

Silk-fibroin from the *B. Mori* cocoon consists of 4.8% tyrosine amino acid [56] and the presence of the other amino acids was also accurately reported [56,57]. Using the molar ratio of the heavy and light chain and P25 protein, we determined the approximate molecular weight of silk-fibroin complex at 194.2 kDa. Therefore, we could calculate an average molecular weight per amino acid, which identified that 102

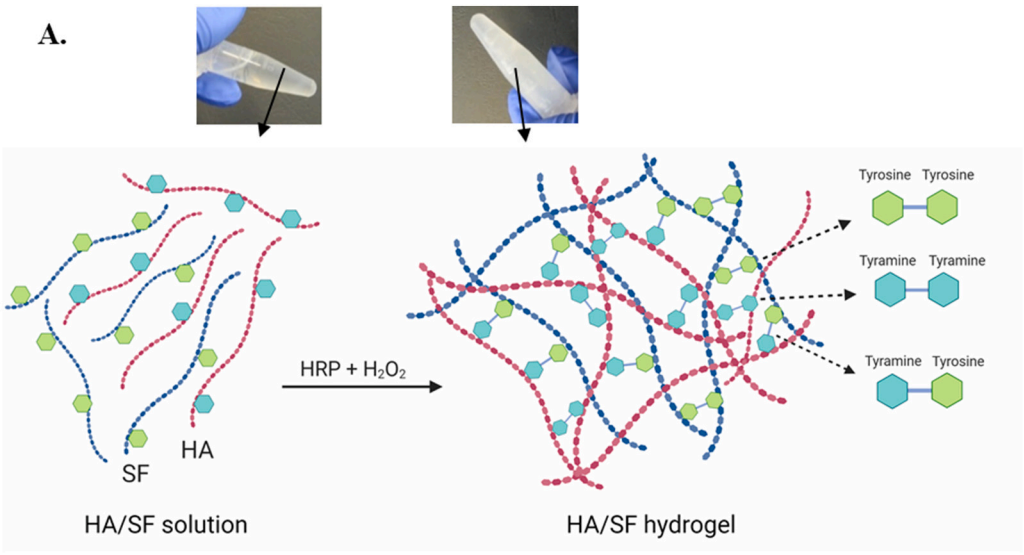


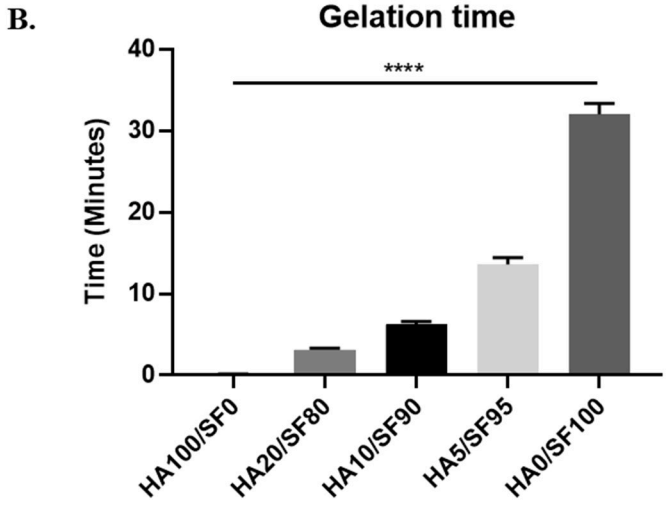


**Fig. 1.** Hydrogel gelation for the HA100/SF0, HA20/SF80, HA10/SF90, HA5/SF95 and HA0/SF100 precursors ($n = 3$). (A) Schematic illustration representing the potential covalent crosslinking in HA-SF composite hydrogels which can occur between tyramine residues of HA and tyrosine in the silk after enzymatic crosslinking. (B) Timing of transition from sol to gel via vial inversion test showed that with increasing HA concentration, the gelation time for the hydrogels was decreased ****$p < 0.0001$.

tyrosine units were present in the silk-fibroin complex. We calculated that 10.50 μM tyrosine is present at a silk-fibroin concentration of 20 mg/mL.

Vial inversion test showed that by increasing the HA-Tyr concentration at a constant fibroin concentration, the gelation time was decreased. The sol-gel transition duration for the pure HA-Tyr hydrogel was the shortest and occurred a few seconds after initiation of enzymatic crosslinking with $H_2O_2$, as assessed by vial inversion test. The slowest sol-gel transition happened for the pure SF hydrogel with a gelation time of approximately 33 min. Conversely, by increasing the HA-Tyr concentration, the gelation time in composite hydrogels was gradually decreasing, with 13, 6 and 3 min for complete gelation of HA5/SF95, HA10/SF90 and HA20/SF80 composite hydrogels, respectively (Fig. 1B).

The physicochemical characterization, enzymatic degradation and the swelling behaviour of the composite hydrogels have previously been reported by Raia et al. [50]. Enzymatic degradation assay showed that HA only hydrogels completely degraded after 6 days in an enzyme solution containing protease and hyaluronidase, while silk only hydrogels maintained 70% of their original weight. With increasing HA concentration, the degradation rate was increasing. We also observed that the degradation rate of HA only hydrogels was much faster in comparison with composite hydrogels. It was furthermore shown that with increasing HA concentration, more water was retained in the hydrogels over time.

### 3.2. Rheological measurements

The rheological measurements indicated that the storage modulus and shear mechanical properties of the hydrogels could be tuned based on the HA-Tyr and SF ratio. The time needed for the hydrogels to reach the maximum mechanical stability due to completed gelation was dependent on the hydrogel precursors ratio. The HA100/SF0 hydrogel reached a final storage modulus in a few minutes, which was significantly faster than HA/SF composite gels. The higher the HA-Tyr proportion in the hydrogel composition was the faster the maximum mechanical stability was achieved. For HA0/SF100 and HA5/SF95 the time to reach the completed crosslinking was between 60 and 75 min, while for HA10/SF90 and HA20/SF80 the time for reaching the complete crosslinking was reduced to 50 and 20 min, respectively (Fig. 2A). Furthermore, the strain sweep showed that HA0/SF100 and HA5/SF95 composite hydrogels could withstand over 100% strain before mechanical failure. By increasing the HA-Tyr concentration in the composite hydrogels the strain at failure was gradually reduced; however, it was significantly higher in composite hydrogels compared to HA100/SF0 hydrogels that started to fail at less than 10% strain (Fig. 2B). Furthermore, the storage modulus for HA100/SF0 hydrogel was the lowest, reaching around 0.32 ± 0.003 kPa; with increasing HA-Tyr

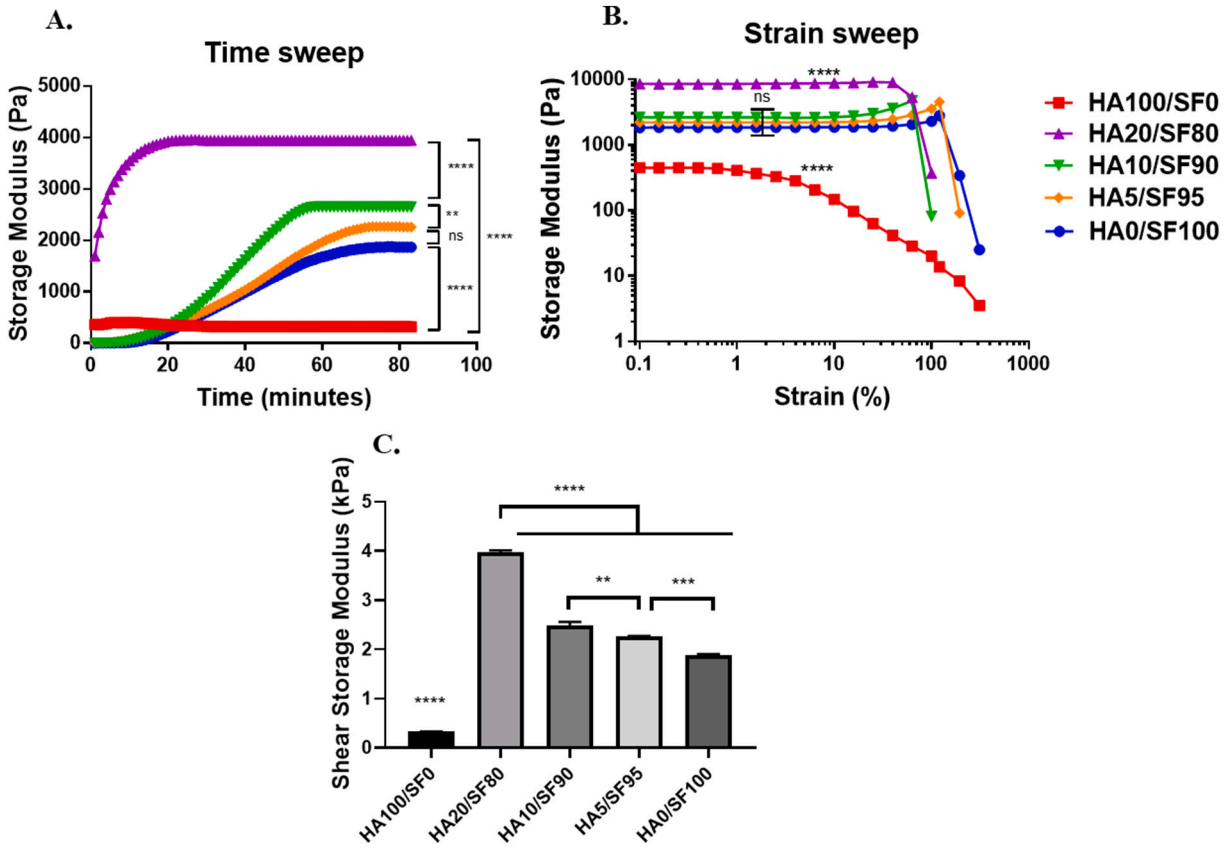


**Fig. 2.** Rheological measurements for the HA100/SF0, HA20/SF80, HA10/SF90, HA5/SF95 and HA0/SF100 hydrogels. (A) Time sweeps showed that HA100/SF0 hydrogels reached the maximum storage faster than other hydrogels and with decreasing HA concentration, the time to reach the final plateau was increased. (B) Strain sweeps determined that the hydrogels with SF in their formulation withstood strains above 100%. Increasing HA concentration gradually lowered strain at failure and HA100/SF0 hydrogels failed at strains above 10%. (C) Final shear storage moduli showed that HA100/SF0 had a lower storage modulus than the hydrogels with SF in their formulation. HA20/SF80 showed the highest storage modulus of all groups. Values are presented as mean ± SD. For statistical analysis one-way analysis of variance (ANOVA) followed by Tukey's post hoc test (multiple comparisons) was applied. ($n = 3$) $^{**}p < 0.001$ $^{***}p < 0.0005$, $^{****}p < 0.0001$, non-significant (ns).

concentration in the composite HA/SF hydrogels, the stiffness increased and reached 3.97 ± 0.02 kPa for HA20/SF80 hydrogels (approx. 10 fold increase) (Fig. 2C).

### 3.3. Chondrocytes viability after encapsulation in hydrogels

To determine the effect of enzymatic crosslinking, hydrogel composition and high density cell encapsulation ($20 \times 10^6$ cells/mL) on cell viability, live-dead assay was performed for the cells encapsulated in HA100/SF0, HA20/SF80 and HA10/SF90 hydrogels at days 1, 3 and 7. Due to the slow gelation of the HA0/SF100 and HA5/SF95 hydrogels, the cells were sedimented on the bottom of the plate and the crosslinking did not take place in these hydrogels in presence of the cells. Therefore, these groups were excluded from our cell-laden experiments. Furthermore, the effect of the culture medium composition (chondrogenic or chondro-permissive medium) on the survival of the cells within the hydrogels was assessed. For the HA20/SF80 cell-laden hydrogels, more than 95% of the chondrocytes cultured in either chondrogenic or chondro-permissive medium were viable at all-time points. Therefore, enzymatic crosslinking did not have any negative effect on cell viability. In HA100/SF0 cell-laden hydrogels, the chondrocytes viability in the chondrogenic medium was slightly decreased from 95% at day 1 to 91% at day 7. Interestingly, for the HA10/SF90 cell-laden hydrogel, the proportion of viable cells in the chondrogenic medium was increased from 93% at day 1 to 98% at day 7, while in the chondro-permissive medium the viable cells were slightly decreased from 90% at day 1 to 86% at day 7. These results showed the effect of TGF-β1 on the chondrocytes viability in HA10/SF90 hydrogel, while in the HA20/SF80 hydrogel the percentage of viable cells was not affected by the cell culture medium composition and the culture period (Fig. 3A–D). Also, we observed that in the HA10/SF90 hydrogel, the chondrocytes appeared elongated, resembling fibroblast-like morphology which may indicate onset of chondrocyte de-differentiation; while HA100/SF0 and HA20/SF80 hydrogels could maintain the rounded chondrogenic morphology of the chondrocytes (Fig. 3E).

### 3.4. Gene expression analysis

To evaluate the effect of the hydrogels' 3D environment and the presence of TGF-β1 on the chondrogenic and pro-inflammatory marker genes, real-time RT-PCR analysis was performed for genes including *COL2AAA1, COL1A2, ACAN, COMP*, *MMP1* and *IL-6* (Fig. 4). The results showed that for all the cell-laden constructs cultured in chondrogenic medium, the expression of *COL2A1* was up-regulated compared with day 0 control (monolayer culture at passage 1), while the *COL2A1* expression in HA20/SF80 hydrogels significantly increased from day 3 to day 7. Additionally, the expression of *COL1A2* was significantly downregulated at day 21 and was lower than day 0 control (below 1) in all hydrogels. The expression of *ACAN* and *COMP* showed a peak at day 7 in HA20/SF80 and was higher than day 0 control in all hydrogels at all-time points. Furthermore, the expression of the catabolic marker gene *MMP1* in HA10/SF90 and HA20/SF80 was significantly down-regulated at day 21 in comparison with day 3. The expression of the pro-inflammatory marker gene *IL-6* was down-regulated compared with day

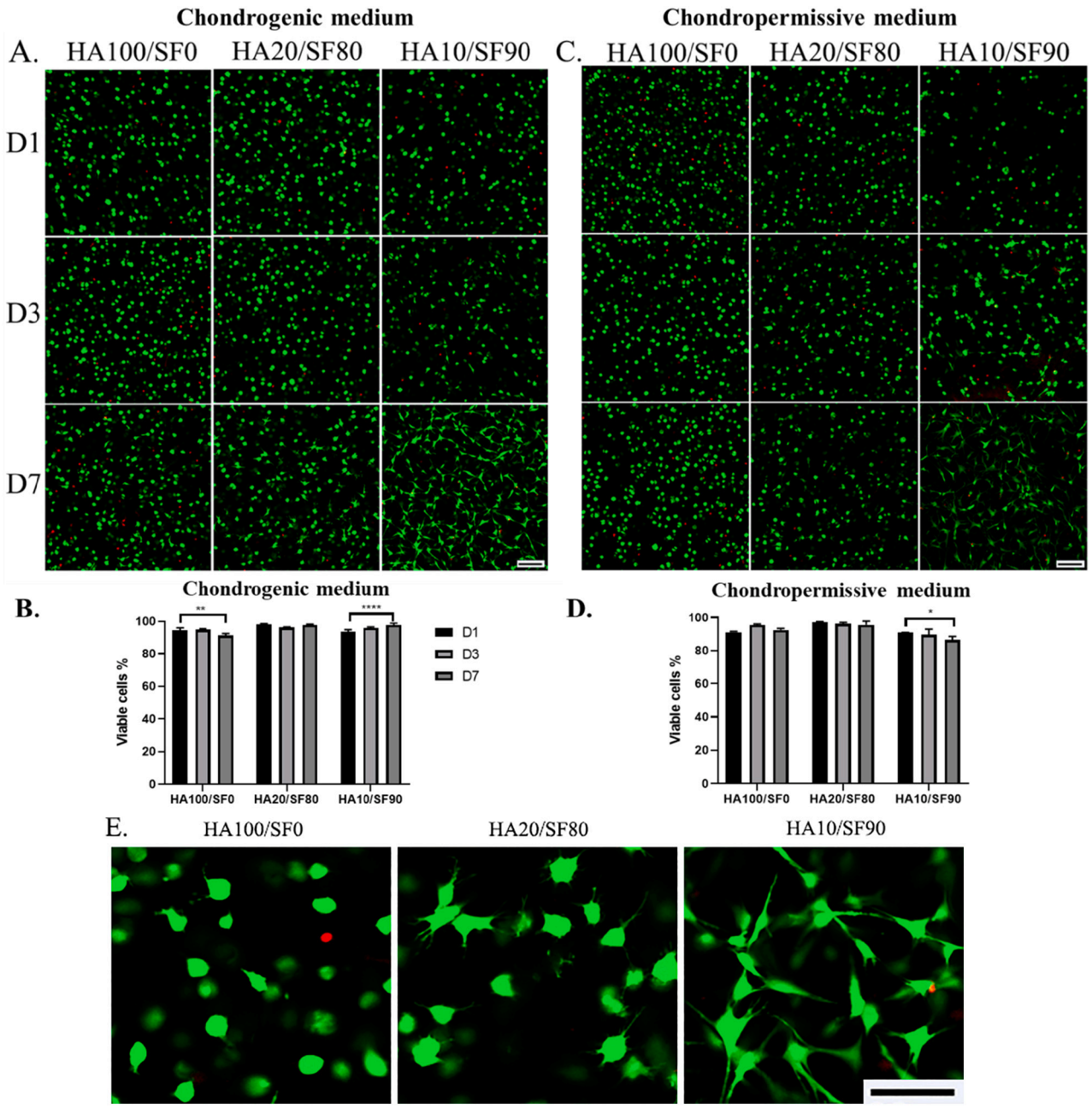


**Fig. 3.** Cell viability for the cell-laden hydrogels (HA100/SF0, HA20/SF80 and HA10/SF90) with live-dead assay at days 1, 3 and 7. (A) Representative confocal images of live/dead stained encapsulated cells within the hydrogels with seeding density of $20 \times 10^6$ cells/mL cultured in chondrogenic medium. Scale bar: 200 μm. (B) Quantification of the cell viability as the percentage of Ca-AM positive cells at days 1, 3 and 7, cultured in chondrogenic medium. (C) Representative confocal images of live/dead stained encapsulated cells within the hydrogels with seeding density of $20 \times 10^6$ cells/mL cultured in chondro-permissive medium. Scale bar: 200 μm (D) Quantification of the cell viability as the percentage of total cells at days 1, 3 and 7, cultured in chondro-permissive medium. Values are presented as mean ± SD from 3 replicates of 2 independent donors and 5 images per group. $^*p < 0.01$, $^{**}p < 0.001$, $^{***}p < 0.0005$ (E) Representative high magnification images showing the morphology of the cells in the hydrogels at day 7 of culture in chondrogenic medium. Scale bar: 100 μm.

0 monolayer culture in all cell-laden hydrogels and showed the lowest levels in HA100/SF0 and HA20/SF80 hydrogels at day 21 (Fig. 4).

For the cell-laden constructs cultured in chondro-permissive medium, the expression of *COL2A1* in HA10/SF90 and HA20/SF80 hydrogels significantly increased during culture time and reached a 10-fold up-regulation at day 21 compared to day 0; while for the HA100/SF0 hydrogel the expression of *COL2A1* did not change over time and was significantly lower than HA10/SF90 and HA20/SF80 hydrogels at day 21. Also, the expression of *COL1A2* was significantly downregulated at day 21 compared with day 3 in all hydrogels. The expression of *ACAN* in HA20/SF80 hydrogels at day 3 was the highest among all groups and timepoints and was reduced gradually by day 21. Furthermore, the expression of *COMP* was significantly increased in HA100/SF0 and HA20/SF80 hydrogels at day 21 compared to earlier time points and compared to *COMP* expression in HA10/SF80 hydrogels. The expression of catabolic and pro-inflammatory marker genes *MMP1* and *IL-6*, normalized to day 0 monolayer culture, was down-regulated (below 1) in all cell-laden hydrogels, and this down-regulation was progressing until day 21 for all cell-laden hydrogels (Fig. 4). Since culturing the cells in both chondrogenic and chondropermissive medium showed the same trend, we used chondrogenic medium in further experiments to assess the potential of the hydrogels to support matrix accumulation.

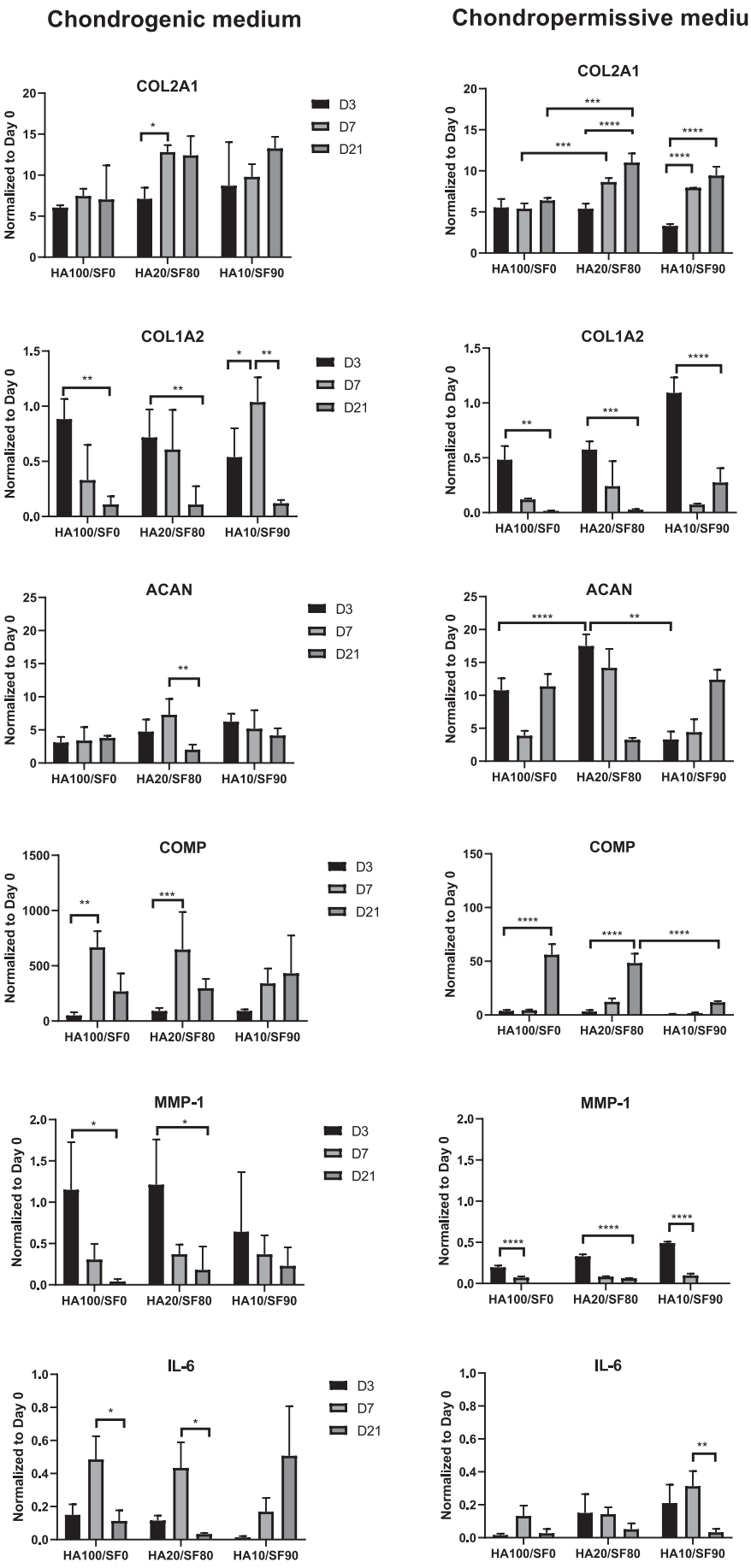
Chondrogenic medium
Chondropermissive medium
COL2A1
COL1A2
ACAN
COMP
MMP-1
IL-6
Normalized to Day 0
D3
D7
D21
HA100/SF0
HA20/SF80
HA10/SF90

**Fig. 4.** Gene expression profile showing transcriptional level of chondrogenic and pro-inflammatory marker genes including *COL2A1, COL1A2, ACAN, COMP, MMP1* and *IL-6* for the cells encapsulated in HA100/SF0, HA20/SF80 and HA10/SF90 at days 3, 7 and 21 cultured in chondrogenic medium and chondropermissive medium in 2 independent donors of bovine chondrocytes; for each donor three experimental replicates were analyzed. Data was normalized to the levels of Day 0 control group. Data are presented as mean ± SD. For statistical analysis using Graphpad Prism 8, one-way analysis of variance (ANOVA) followed by Tukey's post hoc test (multiple comparisons) was applied. $*p < 0.01$, $**p < 0.001$, $***p < 0.0005$, $****p < 0.0001$.

### 3.5. Mechanical testing

Unconfined compressive properties of cell-free and cell-laden constructs including HA100/SF0, HA20/SF80 and HA10/SF90, were determined at days 1, 7, 14, 21 and 28. Initially, at day 1, all hydrogels had compressive moduli ranging between ~1 and 4 kPa with the highest value measured for HA20/SF80 hydrogels. In cell-free constructs, the compressive moduli of all hydrogels remained nearly constant until day 21. However, for HA20/SF80 and HA10/SF90 hydrogels at day 28, the compressive modulus was significantly increased and reached a final modulus of 19.2 ± 1.8 kPa and 16.9 ± 0.2 kPa, respectively, while for HA100/SF0 this value remained unchanged. Therefore, in the cell-free constructs, the significant increase in the compressive modulus of HA20/SF80 and HA10/SF90 was due to the formation of β-sheet secondary structures in SF. After culture of the cell-laden constructs in chondrogenic medium, the compressive modulus of HA20/SF80 hydrogels was significantly higher compared to the other groups (both cell-laden and cell-free) and reached a final compressive modulus of 29.06 ± 3.1 kPa at day 28, which confirmed the significant matrix deposition in this hydrogel. Also, for HA100/SF0 and HA10/SF90 hydrogels, the compressive modulus was increased over time and reached final moduli of 15.9 ± 1.1 kPa and 11.49 ± 0.1 kPa at day 28, respectively (Fig. 5A, B). Further results showed that the percentage of relaxation significantly increased in all cell-laden hydrogels from day 1 to day 7 of culture in chondrogenic medium. The percentage of stress-relaxation was initially highest for HA10/SF90 hydrogels at day 1, and this value was increased over the culture period in all hydrogels (Supplementary Fig. 1).

### 3.6. Histological analysis

To observe matrix deposition in the hydrogels, Safranin-O (Saf—O) and Alcian blue staining were performed for the hydrogel constructs cultured in chondrogenic medium at days 1, 14, 21 and 28. The results showed that sulphated glycosaminoglycans (sGAG) were produced and deposited in all the hydrogels, in the period of 28 days of culture in chondrogenic medium, indicating that the hydrogels supported chondrogenic matrix production (Fig. 6A and Supplementary Fig. 2). In the HA20/SF80 group, we observed higher intensity of Saf-O and Alcian blue staining in comparison with HA10/SF90 and HA100/SF0 hydrogels at different time points. This higher intensity suggests that the cells deposited a higher amount of proteoglycan in the tissue constructs. The immunostaining for COL-2 at day 21 showed that this specific cartilaginous ECM protein was also expressed in all hydrogels. Moreover, we observed that in HA100/SF0 and HA20/SF80 hydrogels, the chondrogenic morphology was maintained, as indicated by the rounded cells residing within the lacuna; while in HA10/SF90 hydrogels, the chondrocytes were not embedded in lacuna and the cells showed a fibroblast-like morphology (Fig. 6B).

### 3.7. Compounds release study

The molecular structures, standard curves, and cumulative release of VA and Epi C from various HA/SF hydrogel compositions at a drug load of 1 mM are shown in Fig. 7. Pure HA-Tyr gels (HA100/SF0) showed very low release of VA (3.0%) and Epi C (7.1%) over the experimental period of 60 days. Composite HA/SF hydrogels showed a substantial increase in drug release that could be observed for both VA and Epi C. When comparing HA20/SF80 and HA10/SF90 hydrogels, a profound difference was seen in VA release, while Epi C release was minimally affected by the SF ratio in the hydrogel. Epi C showed strong burst release during the first week of the release experiment (54.0% for both composite hydrogels), followed by a plateau phase over the rest of the experiment in which less than 1% of the initial drug load was released into the surrounding PBS. The highest cumulative VA release (70.1%) was seen when the compound was embedded in HA20/SF80. Negligible quantities of VA and Epi C were recovered upon overnight enzymatic degradation of the hydrogels at day 60, indicating that possible degradation products of VA and Epi C could have remained unidentified during the HPLC measurements (Fig. 7A–F).

## 4. Discussion

Tunable composite hydrogels for cartilage TE and drug delivery have been introduced in recent years as a desirable alternative to invasive treatments [58,59]. Previous studies investigating HA/SF composite hydrogels showed that HA5/SF95, HA10/SF90 and HA20/SF80 hydrogels formed interconnected hydrogel networks with di-tyramine, di-tyrosine and tyramine-tyrosine bonds [50]. In this work, these composite HA/SF hydrogels were further assessed for their ability to provide an encapsulating matrix for chondrocytes and as carrier material for anti-inflammatory drugs. Initially, the mechanical properties and gelation of the hydrogels were characterized over time. The rheological time sweep showed that due to higher polymer amount in HA20/SF80 hydrogels, more available crosslinking sites were present, and the higher crosslink density (di-tyramine, di-tyrosine and tyramine-tyrosine) resulted in higher storage modulus (4 kPa) compared with other hydrogels in this study (Fig. 2A). Additionally, HA20/SF80 hydrogels had the highest polymer concentration among all tested hydrogels, which also contributed to the high storage modulus. The strain sweep showed that HA0/SF100 and HA5/SF95 composite hydrogels could resist over 100% strain before mechanical failure, and by increasing the HA-Tyr concentration in the composite hydrogels the strain at failure was gradually reduced. However, a significant improvement was observed for the composite hydrogels compared to HA100/SF0 hydrogels that started to fail at less than 10% strain (Fig. 2B). These mechanical properties could make the composite hydrogels suitable for TE of joint cartilage which is normally exposed to physiological loads of approximately 20% strain [60,61]. The duration of gelation of composite HA/SF hydrogels was directly related to the HA-Tyr and SF ratio,

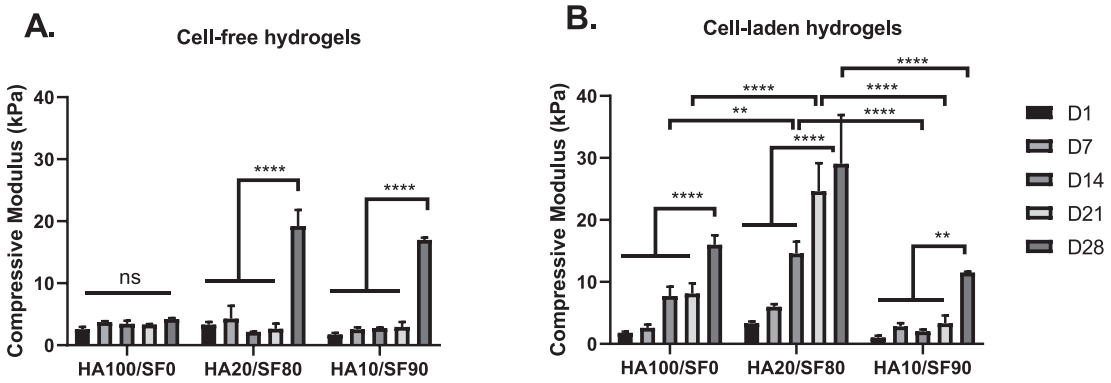


**Fig. 5.** Mechanical testing of HA100/SF0, HA20/SF80, HA10/SF90 cell-free and cell-laden hydrogel constructs at days 1, 7, 14, 21 and 28. (A) Compressive moduli of the cell-free hydrogels over the period of 28 days. (B) Compressive moduli of the cell-laden hydrogels cultured in chondrogenic medium showed most pronounced increase for HA20/SF80 hydrogels. Values are presented as mean ± SD from 3 replicates of 2 independent donors per group. For statistical analysis using Graphpad Prism 8, one-way analysis of variance (ANOVA) followed by Tukey's post hoc test (multiple comparisons) was applied. $^{*}p < 0.01$, $^{**}p < 0.001$, $^{***}p < 0.0005$, $^{****}p < 0.0001$ and ns (non-significant).

corroborating the findings from Raia et al. [50]. The extremely fast gelation of HA100/SF0 and the slow gelation of HA0/SF100 indicate that the crosslinking kinetics of HA and SF materials were different. HA20/SF80 and HA10/SF90 optimized ratios had a gelation time of 3 and 6 min allowing easy handling for clinical applications, including drug or cell loading, prior to injection and setting [62] (Fig. 1A, B). While to our knowledge there is no evidence that, from a chemical standpoint, the formation of di-tyramine bonds is favorable over that of di-tyrosine bonds, there might be a difference in the number of available phenol groups in both polymers. With our synthesized HA showing a tyramine DS of 14% and SF having approximately 5% tyrosine in its heavy chain amino acids [63], an abundance of phenols should be present in all hydrogel groups to facilitate fast enzymatic crosslinking. Another reason for the slower gelation of SF might be the formation of β-sheet structures that reduce the polymer chain mobility.

When assessing the encapsulated drug release from the composite hydrogels, VA was generally released more slowly compared to Epi C (Fig. 7). This was surprising and perhaps counter intuitive due to the much lower molecular weight, and thus increased diffusion kinetics, of VA (Fig. 7A, B). However, as the gels are formed by crosslinking between phenol groups of tyramine and tyrosine, it is possible that crosslinking of the VA phenol group with the hydrogel occurred as well. This hypothesis is supported by the fact that hydrogels with a 10 mM VA load were not able to gel (data not shown). Epi C also has ring structures, but their 3D conformation would result in more steric hindrance, mostly preventing such drug-hydrogel interactions. The covalent C—C bond that can form between VA and tyramine or tyrosine groups is considered stable and is unlikely to provide a sustained release of VA through crosslink degradation. However, ring structures associated with the crosslinked VA could provide physical interactions with encapsulated VA through π-π stacking of their planar aromatic rings. Enzymatic hydrogel degradation with hyaluronidase at the end of the drug release study might not have broken up phenol complexes between tyramine groups and VA, explaining why negligible VA quantities were observed in the endpoint degraded gels. Therefore, to prevent the covalent reaction between VA and tyramine or tyrosine, one could consider encapsulating VA in microparticles that could be added to SF/HA hydrogels. This approach could minimize VA-hydrogel interaction during crosslinking and potentially allow for a slower VA release.

To evaluate the effect of hydrogel composition and stiffness on the ECM deposition, bovine chondrocytes were embedded at high density ($20 \times 10^6$ cells/mL) in enzymatically crosslinked HA/SF composites or HA-Tyr hydrogels. Previous studies with high density cell-laden SF hydrogels showed that such hydrogels were favorable for the redifferentiation of culture-expanded chondrocytes and ECM deposition [64]. However, due to the slow gelation, crosslinking did not occur in HA0/SF100 and HA5/SF95 hydrogels in the presence of high numbers of cells, while composites with the higher percentage of HA (HA20/SF80, HA10/SF90) were crosslinked successfully due to faster gelation [29,65]. HA100/SF0 and HA20/SF80 composite hydrogels could also promote re-differentiation of the chondrocytes by preserving the chondrogenic phenotype, while in HA10/SF90 hydrogels the cells were more elongated. Interestingly, Loebel et al. also showed that after encapsulation of chondrocytes in hydrogels at higher crosslinking densities, the nascent matrix was more restricted to the pericellular space and could not spread into the hydrogel, while in less crosslinked formulations it spread into the hydrogel [66]. Moreover, it was previously shown that different ratios of SF/HA composite hydrogels had different porous structures in which SF80/HA20 hydrogels could promote the formation of spheroids from mesenchymal stem cells (MSCs) which were resembling native cartilage structure, while in SF100/HA0 and SF90/HA10 composite hydrogels, the cells were shown to be more elongated [67]. It was previously shown that with encapsulating high numbers of cells in HA-Tyr hydrogels their mechanical properties were significantly decreased (storage modulus ˂1 kPa) which is not optimal for promoting ECM production by the cells [31,38]. Also, it was shown that by increasing the $H_2O_2$ concentration, stiffer materials could be formed [30,31]. Nevertheless, the small mesh size of highly crosslinked HA-Tyr gels was resulting in insufficient transport of nutrients, restriction of cell growth and prevention of cellular remodeling [30]. We observed that in HA100/SF0 hydrogels in chondrogenic medium, the proportion of viable cells was decreased over time which could be due to the limited transfer of nutrients to the cells encapsulated in the hydrogels. Also, high concentrations of HRP and $H_2O_2$ could increase cytotoxicity and will potentially induce immune responses [32,33]. We showed that in the presence of 0.01% $H_2O_2$ and with a high chondrocyte density, more than 90% of the chondrocytes cultured in chondrogenic medium were viable in all hydrogel formulations. In HA20/SF80 hydrogels more than 95% of the chondrocytes were viable over the culture period in both chondrogenic and chondro-permissive media. This high cell viability verified a proper stiffness of the hydrogels and diffusion of nutrients, providing a favorable environment for the metabolism of the chondrocytes (Fig. 3A, B). Also, the expression of chondrogenic marker genes (*COL2A1, ACAN* and *COMP*) in all chondrocyte-laden constructs was up-regulated compared with the day 0 time point, with up-regulation being most pronounced in HA20/SF80 hydrogels in both chondrogenic and chondro-permissive media. The expression of pro-inflammatory marker genes (*MMP1* and *IL-6*) was down-regulated compared to day 0, which supports the anti-inflammatory properties of SF and HA based hydrogels that were reported previously [20,51]. Furthermore, the ECM deposition was

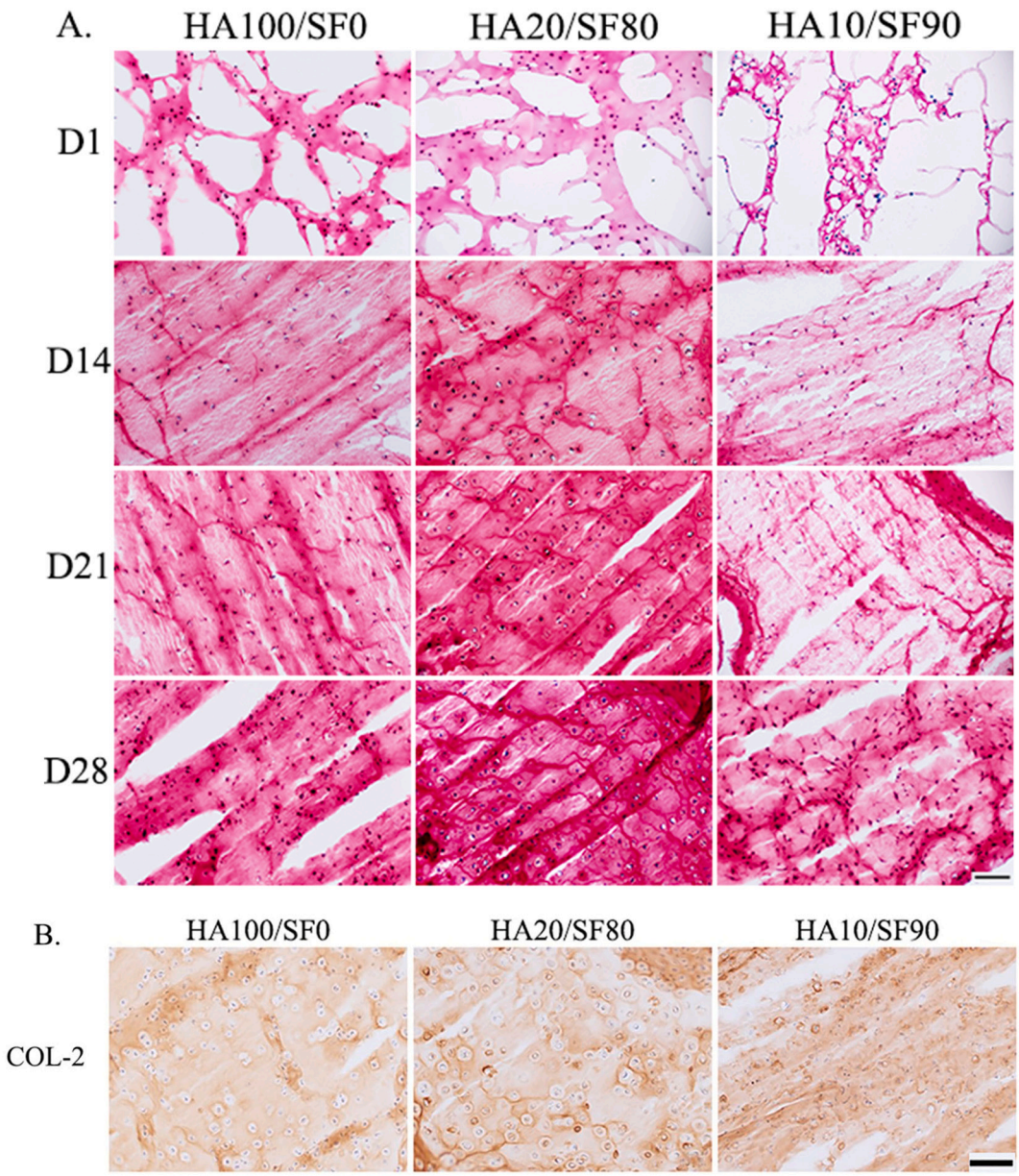


**Fig. 6.** Histological and immunohistochemical characterization of the cell-encapsulated hydrogel constructs including HA100/SF0, HA20/SF80 and HA10/SF90. (A) Safranin-O staining of the hydrogels at days 1, 14, 21 and 28. (B) Immunostaining for COL-2 at day 21 revealed that type II collagen accumulated in all hydrogels and the chondrogenic cell morphology was maintained in HA100/SF0 and HA20/SF80 hydrogels. Scale bars = 100 μm.

increased in all hydrogels over 28 days of culture with the most noticeable increase for HA20/SF80 hydrogels, as characterized by Safranin-O and Alcian blue staining (Fig. 6 and Supplementary Fig. 2).

The unconfined compressive properties showed that the compressive modulus for the HA20/SF80 chondrocyte-laden constructs was significantly increased over 28 days of culture in chondrogenic medium. This higher level of compressive modulus was likely due to both the superior matrix deposition in HA20/SF80 hydrogels, and the intrinsic features of the HA/SF hydrogels which were getting stiffer over time, most probably due to the formation of β-sheet secondary structures in SF. The hydrogel stiffening in cell-free HA/SF composite hydrogels was significant from day 21 to day 28 which was likely due to the evolution of silk-fibroin secondary structures (β-sheet). The lower compression moduli achieved in our study compared to the study by Raia et al. [50] could be due to the different quality of the processed silk fibroin and/or the lower strain (20% vs 30%) applied in our study [68,69]. Moreover, encapsulated cells can strongly influence the bulk mechanical properties of the hydrogels, and the chemical crosslinking is weaker in presence of encapsulated cells than in the absence of embedded cells. Here, we showed that by embedding cells in HA/SF hydrogels, the compression moduli were further increased over time (at different time points), which confirmed the accumulation of matrix in presence of the cells in the composite hydrogels. In HA100/SF0 and HA20/SF80 cell-laden constructs, there was a gradual increase in compressive modulus from day 1 to day 28 due to the matrix deposition, whereby this increase was significantly higher in HA20/SF80 hydrogels. However, in HA10/SF90 hydrogels, we did not observe an increasing trend in stiffness from day 1 to day 21, while there was a rise at day 28 similar to cell-free hydrogels. This may indicate that the matrix deposition was not considerable in these hydrogels and the observed increase at day 28 was due to the formation of β-sheet structures. Also, it is known that adherent cells like chondrocytes sense the viscoelasticity of their surrounding environment and the stiffness of the matrix can influence contractility and spreading of the cells [70]. Therefore, there is a feedback loop of physical and

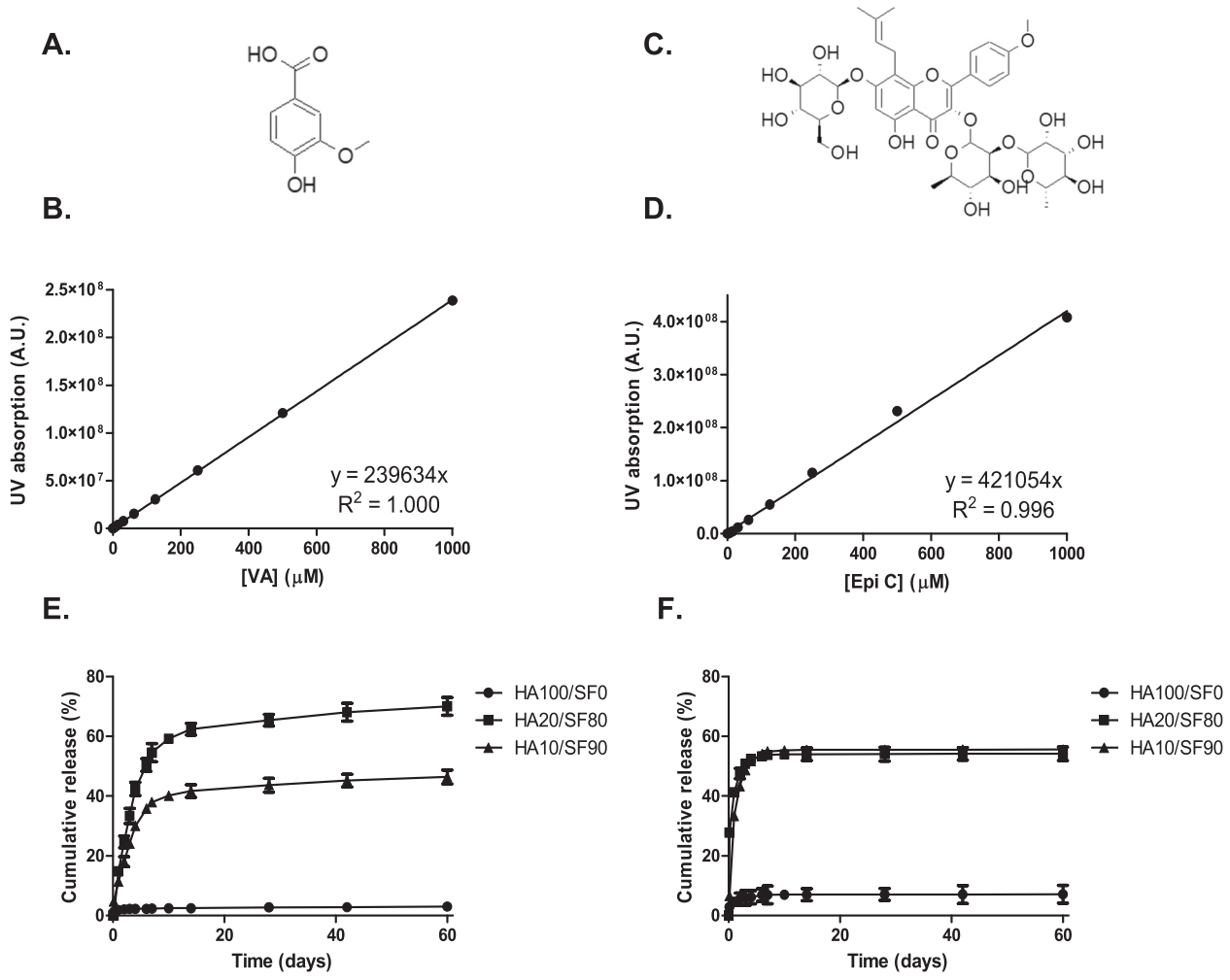


**Fig. 7.** Release study for the compounds loaded in HA100/SF0, HA20/SF80 and HA10/SF90 hydrogels. Molecular structure of (A) VA and (C) Epi C. Standard curves of (B) VA and (D) Epi C in PBS. Cumulative release profiles of (E) VA and (F) Epi C from HA and HA/SF composite hydrogels.

biochemical signals in response to the elasticity of the extracellular microenvironment which influences cell fate and morphology [71]. In this study, we showed that HA20/SF80 could provide the most adequate environment for the chondrocytes to re-differentiate and deposit ECM to reach mechanical and biological properties which can resemble the native cartilage [68].

Lee et al. showed that in fast relaxing hydrogels which dissipate elastic stresses more quickly, chondrocytes tend to form interconnected regions of ECM, while in slow relaxing hydrogels, elastic stresses restrict cell movement and growth which limits chondrocyte matrix production [72]. In this study, we observed that in the cell-laden HA100/SF0 and HA20/SF80 hydrogels, the percentage of the stress relaxation was significantly increased from day 1 to day 7, which was due to the matrix deposition in the hydrogels. These results highlight the impact of controlled change of hydrogel mechanical properties over time on cell differentiation and fate. In this regard, HA100/SF0 and HA20/SF80 showed suitable moderate elastic properties in the initial phase of the cell culture that diminished over time.

Furthermore, HA100/SF0 hydrogels were very fast degradable and these hydrogels were degraded over the period of culture, while composite hydrogels remained intact till the end of the culture period at 28 days (data not shown). It has been shown that scaffolds more resistant to degradation supported the matrix production by chondrocytes for a longer period, making them suitable for ex vivo and in vivo applications [73]. Therefore, the degradation rate of hydrogels and their potential in supporting cell maturation and matrix deposition should be evaluated in further ex vivo and in vivo studies.

Due to the limited number of human chondrocytes from biopsies, several monolayer passages are usually necessary before utilization for TE studies [55]. In this study, minimally expanded bovine chondrocytes were used to prevent the use of de-differentiated cells due to cell expansion. However, this source of cells has limited relevance for further pre-clinical and clinical applications, and the utilization of other sources of cells including human articular chondrocytes, MSCs and nasal chondrocytes are envisioned [31,74]. In addition, besides collagen II, the synthesis of other ECM proteins, especially collagen type I, should be analyzed in further studies, to confirm the generation of a hyaline cartilaginous ECM within the hydrogel. Finally, previous studies showed that mechanical stimulation was necessary for promoting ECM production in chondrocytes and MSCs [31,75]. Since our hydrogels showed mechanical properties suitable for withstanding mechanical loads, the mechanobiology of the chondrocytes encapsulated in the HA20/SF80 hydrogel in response to mechanical compression and shear should be evaluated in future experiments using a cartilage bioreactor system as established by our group [76].

In conclusion, with the enzymatic crosslinking of SF and HA-Tyr solutions, we developed an injectable and tunable composite hydrogel for cartilage TE and drug delivery purposes. We demonstrated that all hydrogels were cytocompatible and that HA100/SF0 and HA20/SF80 composite hydrogels could preserve the chondrogenic phenotype through increased expression of chondrogenic marker genes and ECM production. Also, the unconfined compressive modulus for the HA20/

SF80 chondrocyte-laden constructs was significantly increased over 28 days of culture in chondrogenic medium, confirming the superior ECM deposition in this composite hydrogel. Furthermore, in the drug loaded hydrogels, HA20/SF80 hydrogel showed the longest and the most sustained release profile for VA and Epi C over time, which is necessary for the long treatment duration for injured or diseased joints. Future in vivo studies using cartilage degeneration models should assess whether the release of VA and/or Epi C is effective in counteracting inflammation and promoting chondrocyte ECM production.

Supplementary data to this article can be found online at https://doi.org/10.1016/j.msec.2020.111701.

## Funding

The study was funded by the AO Foundation and by the Swiss National Science Foundation (SNF) under the SSSTC program with grant number 156362.

## CRediT authorship contribution statement

**Reihane Ziadlou:** Conceptualization, Data curation, Formal analysis, Investigation, Methodology, Validation, Visualization, Writing - original draft, Writing - review & editing. **Stijn Rotman:** Conceptualization, Data curation, Formal analysis, Investigation, Methodology, Writing - original draft, Writing - review & editing. **Andreas Teuschl:** Investigation, Methodology, Resources, Writing - review & editing. **Elias Salzer:** Investigation, Methodology, Writing - review & editing. **Andrea Barbero:** Conceptualization, Investigation, Methodology, Supervision, Writing - review & editing. **Ivan Martin:** Conceptualization, Investigation, Methodology, Supervision, Writing - review & editing. **Mauro Alini:** Conceptualization, Funding acquisition, Investigation, Project administration, Resources, Supervision, Writing - review & editing. **David Eglin:** Conceptualization, Formal analysis, Funding acquisition, Investigation, Methodology, Project administration, Resources, Supervision, Writing - review & editing. **Sibylle Grad:** Conceptualization, Formal analysis, Funding acquisition, Investigation, Methodology, Project administration, Resources, Supervision, Writing - review & editing.

## Declaration of competing interest

The authors declare that they have no known competing financial interests or personal relationships that could have appeared to influence the work reported in this paper.

## Acknowledgments

We would like to acknowledge Mauro Bluvol and Nora Goudsouzian for their technical support with histology. Also, we would like to thank Dominic Mischler, Peter Varga, Ivan Zderic and Dieter Wahl for their technical support with Instron mechanical testing.

## References

[1] Krishnan Y, Grodzinsky AJ. Cartilage diseases. Matrix Biol. 2018;71–72:51–69.
[2] Poole AR, Kojima T, Yasuda T, Mwale F, Kobayashi M, Laverty S. Composition and structure of articular cartilage: a template for tissue repair. Clin Orthop Relat Res. 2001(391 Suppl):S26–33.
[3] R.F. Loeser, Age-related changes in the musculoskeletal system and the development of osteoarthritis, Clin. Geriatr. Med. 26 (3) (2010) 371–386.
[4] B. Heidari, Knee osteoarthritis prevalence, risk factors, pathogenesis and features: part I, Caspian J Intern Med. 2 (2) (2011) 205–212.
[5] L.J. Sandell, T. Aigner, Articular cartilage and changes in arthritis: cell biology of osteoarthritis, Arthritis research & therapy. 3 (2) (2001) 107.
[6] T. Minas, T. Ogura, T. Bryant, Autologous chondrocyte implantation, JBJS Essent Surg Tech. 6 (2) (2016), e24.
[7] S. Gortz, W.D. Bugbee, Allografts in articular cartilage repair, Instr. Course Lect. 56 (2007) 469–480.
[8] V. Wylde, A. Beswick, J. Bruce, A. Blom, N. Howells, R. Gooberman-Hill, Chronic pain after total knee arthroplasty, EFORT Open Rev. 3 (8) (2018) 461–470.
[9] S. Roberts, J. Menage, L.J. Sandell, E.H. Evans, J.B. Richardson, Immunohistochemical study of collagen types I and II and procollagen IIA in human cartilage repair tissue following autologous chondrocyte implantation, Knee. 16 (5) (2009) 398–404.
[10] M. Liu, X. Zeng, C. Ma, H. Yi, Z. Ali, X. Mou, et al., Injectable hydrogels for cartilage and bone tissue engineering, Bone Research. 5 (1) (2017) 17014.
[11] S.L. Vega, M.Y. Kwon, J.A. Burdick, Recent advances in hydrogels for cartilage tissue engineering, Eur Cell Mater. 33 (2017) 59–75.
[12] W.S. Toh, M. Spector, E.H. Lee, T. Cao, Biomaterial-mediated delivery of microenvironmental cues for repair and regeneration of articular cartilage, Mol. Pharm. 8 (4) (2011) 994–1001.
[13] A.S. Hoffman, Hydrogels for biomedical applications, Adv. Drug Deliv. Rev. 64 (2012) 18–23.
[14] H.M. Pauly, L.W. Place, T.L. Haut Donahue, M.J. Kipper, Mechanical properties and cell compatibility of agarose hydrogels containing proteoglycan mimetic graft copolymers, Biomacromolecules. 18 (7) (2017) 2220–2229.
[15] A.D. Augst, H.J. Kong, D.J. Mooney, Alginate hydrogels as biomaterials, Macromol. Biosci. 6 (8) (2006) 623–633.
[16] K.Y. Lee, D.J. Mooney, Alginate: properties and biomedical applications, Prog. Polym. Sci. 37 (1) (2012) 106–126.
[17] E.E. Antoine, P.P. Vlachos, M.N. Rylander, Review of collagen I hydrogels for bioengineered tissue microenvironments: characterization of mechanics, structure, and transport, Tissue Eng. B Rev. 20 (6) (2014) 683–696.
[18] G.Z. Jin, H.W. Kim, Efficacy of collagen and alginate hydrogels for the prevention of rat chondrocyte dedifferentiation, Journal of tissue engineering. 9 (2018) (2041731418802438).
[19] L. Li, F. Yu, L. Zheng, R. Wang, W. Yan, Z. Wang, et al., Natural hydrogels for cartilage regeneration: modification, preparation and application, Journal of orthopaedic translation. 17 (2019) 26–41.
[20] K. Masuko, M. Murata, K. Yudoh, T. Kato, H. Nakamura, Anti-inflammatory effects of hyaluronan in arthritis therapy: not just for viscosity, International journal of general medicine. 2 (2009) 77–81.
[21] M. Akmal, A. Singh, A. Anand, A. Kesani, N. Aslam, A. Goodship, et al., The effects of hyaluronic acid on articular chondrocytes, The Journal of bone and joint surgery British volume. 87 (8) (2005) 1143–1149.
[22] E.J. Jansen, P.J. Emans, C.M. Douw, N.A. Guldemond, L.W. Van Rhijn, S.K. Bulstra, et al., One intra-articular injection of hyaluronan prevents cell death and improves cell metabolism in a model of injured articular cartilage in the rabbit, Journal of orthopaedic research : official publication of the Orthopaedic Research Society. 26 (5) (2008) 624–630.
[23] T. Yasuda, Hyaluronan inhibits prostaglandin E2 production via CD44 in U937 human macrophages, Tohoku J. Exp. Med. 220 (3) (2010) 229–235.
[24] A. Roth, J. Mollenhauer, A. Wagner, R. Fuhrmann, A. Straub, R.A. Venbrocks, et al., Intra-articular injections of high-molecular-weight hyaluronic acid have biphasic effects on joint inflammation and destruction in rat antigen-induced arthritis, Arthritis research & therapy. 7 (3) (2005) R677–R686.
[25] F. Lee, J.E. Chung, M. Kurisawa, An injectable hyaluronic acid-tyramine hydrogel system for protein delivery, Journal of controlled release : official journal of the Controlled Release Society. 134 (3) (2009) 186–193.
[26] Kurisawa M, Chung JE, Yang YY, Gao SJ, Uyama H. Injectable biodegradable hydrogels composed of hyaluronic acid-tyramine conjugates for drug delivery and tissue engineering. Chemical communications (Cambridge, England). 2005(34): 4312–4.
[27] W.S. Toh, T.C. Lim, M. Kurisawa, M. Spector, Modulation of mesenchymal stem cell chondrogenesis in a tunable hyaluronic acid hydrogel microenvironment, Biomaterials. 33 (15) (2012) 3835–3845.
[28] K.S. Kim, S.J. Park, J.A. Yang, J.H. Jeon, S.H. Bhang, B.S. Kim, et al., Injectable hyaluronic acid–tyramine hydrogels for the treatment of rheumatoid arthritis, Acta Biomater. 7 (2) (2011) 666–674.
[29] L. Sherman, J. Sleeman, P. Herrlich, H. Ponta, Hyaluronate receptors: key players in growth, differentiation, migration and tumor progression, Curr. Opin. Cell Biol. 6 (5) (1994) 726–733.
[30] C. Loebel, T. Stauber, M. D'Este, M. Alini, M. Zenobi-Wong, D. Eglin, Fabrication of cell-compatible hyaluronan hydrogels with a wide range of biophysical properties through high tyramine functionalization, J. Mater. Chem. B 5 (12) (2017) 2355–2363.
[31] P. Behrendt, Y. Ladner, M.J. Stoddart, S. Lippross, M. Alini, D. Eglin, et al., Articular joint-simulating mechanical load activates endogenous TGF-β in a highly cellularized bioadhesive hydrogel for cartilage repair, Am. J. Sports Med. 48 (1) (2020) 210–221.
[32] T. Sminia, F. Delemarre, E.M. Janse, Histological observations on the intestinal immune response towards horseradish peroxidase in rats, Immunology. 50 (1) (1983) 53–56.
[33] A.M. Gardner, F.H. Xu, C. Fady, F.J. Jacoby, D.C. Duffey, Y. Tu, et al., Apoptotic vs. nonapoptotic cytotoxicity induced by hydrogen peroxide, Free Radic. Biol. Med. 22 (1–2) (1997) 73–83.
[34] K.L. Spiller, S.A. Maher, A.M. Lowman, Hydrogels for the repair of articular cartilage defects, Tissue Eng. B Rev. 17 (4) (2011) 281–299.
[35] S. Bhumiratana, R.E. Eton, S.R. Oungoulian, L.Q. Wan, G.A. Ateshian, G. Vunjak-Novakovic, Large, stratified, and mechanically functional human cartilage grown in vitro by mesenchymal condensation, Proc. Natl. Acad. Sci. U. S. A. 111 (19) (2014) 6940–6945.
[36] R. Stern, G. Kogan, M.J. Jedrzejas, L. Soltes, The many ways to cleave hyaluronan, Biotechnol. Adv. 25 (6) (2007) 537–557.

[37] E.B. Hunziker, Articular cartilage repair: basic science and clinical progress. A review of the current status and prospects, Osteoarthr. Cartil. 10 (6) (2002) 432–463.
[38] L.S. Wang, C. Du, W.S. Toh, A.C. Wan, S.J. Gao, M. Kurisawa, Modulation of chondrocyte functions and stiffness-dependent cartilage repair using an injectable enzymatically crosslinked hydrogel with tunable mechanical properties, Biomaterials. 35 (7) (2014) 2207–2217.
[39] T. Yucel, M.L. Lovett, D.L. Kaplan, Silk-based biomaterials for sustained drug delivery, Journal of controlled release : official journal of the Controlled Release Society. 190 (2014) 381–397.
[40] B.P. Partlow, C.W. Hanna, J. Rnjak-Kovacina, J.E. Moreau, M.B. Applegate, K. A. Burke, et al., Highly tunable elastomeric silk biomaterials, Adv. Funct. Mater. 24 (29) (2014) 4615–4624.
[41] D.N. Rockwood, R.C. Preda, T. Yucel, X. Wang, M.L. Lovett, D.L. Kaplan, Materials fabrication from Bombyx mori silk fibroin, Nat. Protoc. 6 (10) (2011) 1612–1631.
[42] G. Cheng, Z. Davoudi, X. Xing, X. Yu, X. Cheng, Z. Li, et al., Advanced silk fibroin biomaterials for cartilage regeneration, ACS Biomaterials Science & Engineering. 4 (8) (2018) 2704–2715.
[43] O. Hasturk, K.E. Jordan, J. Choi, D.L. Kaplan, Enzymatically crosslinked silk and silk-gelatin hydrogels with tunable gelation kinetics, mechanical properties and bioactivity for cell culture and encapsulation, Biomaterials. 232 (2020) 119720.
[44] C. Vepari, D.L. Kaplan, Silk as a biomaterial, Prog. Polym. Sci. 32 (8–9) (2007) 991–1007.
[45] L. Lamboni, M. Gauthier, G. Yang, Q. Wang, Silk sericin: a versatile material for tissue engineering and drug delivery, Biotechnol. Adv. 33 (8) (2015) 1855–1867.
[46] B.P. Partlow, M. Bagheri, J.L. Harden, D.L. Kaplan, Tyrosine templating in the self-assembly and crystallization of silk fibroin, Biomacromolecules. 17 (11) (2016) 3570–3579.
[47] J. Chen, Y. Zhan, Y. Wang, D. Han, B. Tao, Z. Luo, et al., Chitosan/silk fibroin modified nanofibrous patches with mesenchymal stem cells prevent heart remodeling post-myocardial infarction in rats, Acta Biomater. 80 (2018) 154–168.
[48] S. Yan, G. Han, Q. Wang, S. Zhang, R. You, Z. Luo, et al., Directed assembly of robust and biocompatible silk fibroin/hyaluronic acid composite hydrogels, Compos. Part B 176 (2019) 107204.
[49] M.H. Kim, B.S. Kim, J. Lee, D. Cho, O.H. Kwon, W.H. Park, Silk fibroin/hydroxyapatite composite hydrogel induced by gamma-ray irradiation for bone tissue engineering, Biomaterials Research. 21 (1) (2017) 12.
[50] N.R. Raia, B.P. Partlow, M. McGill, E.P. Kimmerling, C.E. Ghezzi, D.L. Kaplan, Enzymatically crosslinked silk-hyaluronic acid hydrogels, Biomaterials. 131 (2017) 58–67.
[51] B. Crivelli, S. Perteghella, E. Bari, M. Sorrenti, G. Tripodo, T. Chlapanidas, et al., Silk nanoparticles: from inert supports to bioactive natural carriers for drug delivery, Soft Matter 14 (4) (2018) 546–557.
[52] C. Loebel, M. D'Este, M. Alini, M. Zenobi-Wong, D. Eglin, Precise tailoring of tyramine-based hyaluronan hydrogel properties using DMTMM conjugation, Carbohydr. Polym. 115 (2015) 325–333.
[53] S. Grad, S. Gogolewski, M. Alini, M.A. Wimmer, Effects of simple and complex motion patterns on gene expression of chondrocytes seeded in 3D scaffolds, Tissue Eng. 12 (11) (2006) 3171–3179.
[54] K.J. Livak, T.D. Schmittgen, Analysis of relative gene expression data using real-time quantitative PCR and the 2(−Delta Delta C(T)) Method, Methods. 25 (4) (2001) 402–408.
[55] Ziadlou R, Barbero A, Stoddart MJ, Wirth M, Li Z, Martin I, et al. Regulation of inflammatory response in human osteoarthritic chondrocytes by novel herbal small molecules. Int J Mol Sci. 2019;20(22).
[56] T. Asakura, K. Suita, T. Kameda, S. Afonin, A.S. Ulrich, Structural role of tyrosine in Bombyx mori silk fibroin, studied by solid-state NMR and molecular mechanics on a model peptide prepared as silk I and II, Magn. Reson. Chem. 42 (2) (2004) 258–266.
[57] S. Inoue, K. Tanaka, F. Arisaka, S. Kimura, K. Ohtomo, S. Mizuno, Silk fibroin of Bombyx mori is secreted, assembling a high molecular mass elementary unit consisting of H-chain, L-chain, and P25, with a 6:6:1 molar ratio, J. Biol. Chem. 275 (51) (2000) 40517–40528.
[58] J. Elisseeff, Injectable cartilage tissue engineering, Expert. Opin. Biol. Ther. 4 (12) (2004) 1849–1859.
[59] J.D. Kretlow, L. Klouda, A.G. Mikos, Injectable matrices and scaffolds for drug delivery in tissue engineering, Adv. Drug Deliv. Rev. 59 (4–5) (2007) 263–273.
[60] C.G. Armstrong, A.S. Bahrani, D.L. Gardner, In vitro measurement of articular cartilage deformations in the intact human hip joint under load, J. Bone Joint Surg. Am. 61 (5) (1979) 744–755.
[61] S. Park, C.T. Hung, G.A. Ateshian, Mechanical response of bovine articular cartilage under dynamic unconfined compression loading at physiological stress levels, Osteoarthr. Cartil. 12 (1) (2004) 65–73.
[62] L.S. Moreira Teixeira, J. Feijen, C.A. van Blitterswijk, P.J. Dijkstra, M. Karperien, Enzyme-catalyzed crosslinkable hydrogels: emerging strategies for tissue engineering, Biomaterials. 33 (5) (2012) 1281–1290.
[63] M. McGill, J.M. Grant, D.L. Kaplan, Enzyme-mediated conjugation of peptides to silk fibroin for facile hydrogel functionalization, Ann. Biomed. Eng. 48 (7) (2020) 1905–1915.
[64] Y. Wang, D.J. Blasioli, H.J. Kim, H.S. Kim, D.L. Kaplan, Cartilage tissue engineering with silk scaffolds and human articular chondrocytes, Biomaterials. 27 (25) (2006) 4434–4442.
[65] A. Aruffo, I. Stamenkovic, M. Melnick, C.B. Underhill, B. Seed, CD44 is the principal cell surface receptor for hyaluronate, Cell. 61 (7) (1990) 1303–1313.
[66] Loebel C, Kwon MY, Wang C, Han L, Mauck RL, Burdick JA. Metabolic labeling to probe the spatiotemporal accumulation of matrix at the chondrocyte–hydrogel interface. Advanced Functional Materials.n/a(n/a):1909802.
[67] J. Jaipaew, P. Wangkulangkul, J. Meesane, P. Raungrut, P. Puttawibul, Mimicked cartilage scaffolds of silk fibroin/hyaluronic acid with stem cells for osteoarthritis surgery: morphological, mechanical, and physical clues, Mater. Sci. Eng. C Mater. Biol. Appl. 64 (2016) 173–182.
[68] J.M. Patel, B.C. Wise, E.D. Bonnevie, R.L. Mauck, A systematic review and guide to mechanical testing for articular cartilage tissue engineering, Tissue engineering Part C, Methods. 25 (10) (2019) 593–608.
[69] S. Park, R. Krishnan, S.B. Nicoll, G.A. Ateshian, Cartilage interstitial fluid load support in unconfined compression, J. Biomech. 36 (12) (2003) 1785–1796.
[70] Discher DE, Janmey P, Wang YL. Tissue cells feel and respond to the stiffness of their substrate. Science (New York, NY). 2005;310(5751):1139–43.
[71] V. Vogel, M. Sheetz, Local force and geometry sensing regulate cell functions, Nat. Rev. Mol. Cell Biol. 7 (4) (2006) 265–275.
[72] H.P. Lee, L. Gu, D.J. Mooney, M.E. Levenston, O. Chaudhuri, Mechanical confinement regulates cartilage matrix formation by chondrocytes, Nat. Mater. 16 (12) (2017) 1243–1251.
[73] M. Sarem, N. Arya, M. Heizmann, A.T. Neffe, A. Barbero, T.P. Gebauer, et al., Interplay between stiffness and degradation of architectured gelatin hydrogels leads to differential modulation of chondrogenesis in vitro and in vivo, Acta Biomater. 69 (2018) 83–94.
[74] Mumme M, Barbero A, Miot S, Wixmerten A, Feliciano S, Wolf F, et al. Nasal chondrocyte-based engineered autologous cartilage tissue for repair of articular cartilage defects: an observational first-in-human trial. Lancet (London, England). 2016;388(10055):1985–94.
[75] Z. Li, S. Yao, M. Alini, S. Grad, Different response of articular chondrocyte subpopulations to surface motion, Osteoarthr. Cartil. 15 (9) (2007) 1034–1041.
[76] S. Grad, C.R. Lee, M.A. Wimmer, M. Alini, Chondrocyte gene expression under applied surface motion, Biorheology. 43 (2006) 259–269.